Increased myofilament calcium sensitivity is associated with decreased cardiac troponin I phosphorylation in the diabetic rat heart

Angela Greenman
University of Otago - Dunedin Campus: University of Otago https://orcid.org/0000-0003-0948-8885
Gary M. Diffee
University of Wisconsin-Madison
Amelia Power
University of Otago - Dunedin Campus: University of Otago
Gerard T. Wilkins
University of Otago - Dunedin Campus: University of Otago
Olivia M. S. Gold
University of Otago - Dunedin Campus: University of Otago
Jeff R. Erickson
University of Otago - Dunedin Campus: University of Otago
James C. Baldi (chris.baldi@otago.ac.nz)
Otago Medical School, University of Otago

Original investigation

Keywords: Myofilament function, diabetes, heart failure, phosphorylation, O-GlcNAcylation

Posted Date: January 29th, 2021

DOI: https://doi.org/10.21203/rs.3.rs-154492/v1

Version of Record: A version of this preprint was published at Experimental Physiology on October 25th, 2021. See the published version at https://doi.org/10.1113/EP089730.

Abstract

Background The diabetic heart has impaired systolic and diastolic function independent of other comorbidities. The availability of calcium is altered, but does not fully explain the cardiac dysfunction seen in the diabetic heart. Thus, we explored if myofilament protein regulation of contraction is altered. Methods Calcium sensitivity (pCa50) was measured in Zucker Diabetic Fatty (ZDF) rat hearts at the initial stage of diabetes (12-week-old) and after 8 weeks of uncontrolled hyperglycaemia (20-week-old) and in non-diabetic (nDM) littermates. Skinned cardiomyocytes were connected to a capacitance-gauge transducer and a torque motor to measure force as a function of pCa (-log[Ca2+]). Fluorescent gel stain (ProQ Diamond) was used to measure total protein phosphorylation. Specific phospho-sites on cardiac troponin I (cTnI) and total cTnI O-GlcNAcylation were quantified using immunoblot. Results pCa50 was greater in both 12- and 20-week-old diabetic (DM) rats compared to nDM littermates ($p = 0.0005$). Total cTnI and cTnI serine 23/24 phosphorylation were lower in DM rats ($p = 0.003$ & $p = 0.01$, respectively), but cTnI O-GlcNAc protein expression was not different. pCa50 is greater in DM rats and corresponds with an overall reduction in cTnI phosphorylation. Conclusions These findings indicate that myofilament calcium sensitivity is increased and cTnI phosphorylation is reduced in ZDF DM rats, which suggests an important role for cTnI phosphorylation in the DM heart.

Background

Diabetes independently impairs left ventricular diastolic (1–6) and systolic (7–10) function and may predispose people to ischaemic disease (10, 11) and heart failure (12–14). One way that diabetes might affect these changes is by altering excitation-contraction coupling (15, 16). The magnitude and duration of the calcium transient (17, 18) and rates of calcium reuptake (19) are reduced in diabetic rat hearts. These changes are often explained by a reduction in the expression of the sarcoplasmic reticulum calcium ATPase pump (SERCA) relative to the SERCA inhibitor phospholamban (PLB). However, right atrial trabeculae from human diabetic biopsies have reduced rates of relaxation and increased duration of relaxation, despite *increased* SERCA/PLB expression (20). In addition, trabecular developed force and maximal rates of contraction were restored without evidence of improved calcium flux (e.g., the calcium transient, calcium decay and total sarcoplasmic calcium content) after inhibition of calcium/calmodulin-dependent protein kinase (CaMKII) in Zucker Diabetic Fatty rat hearts (21). These data indicate that impaired relaxation and contractile function of the diabetic heart cannot be fully explained by deranged excitation-contraction coupling.

An additional explanation may be that the affinity of calcium bound to cardiac troponin, or the calcium sensitivity of the myofilaments, is altered by diabetes. Post-translational phosphorylation of myofilament proteins, particularly cTnI (22, 23) and cardiac myosin binding protein C (cMyBP-C) (24) alter the calcium sensitivity of force (pCa_{50}) in 'skinned' (membrane removed) cardiomyocyte preparations. Specific phospho-sites on cTnI (e.g., serine (Ser)23/24) and the resultant changes in calcium sensitivity are implicated in heart failure (25), but these associations have not been established in the diabetic heart.

Jweied and colleagues showed that calcium sensitivity was reduced in human diabetic cardiomyocytes and that cardiac troponin I (cTnI) and cardiac troponin T (cTnT) phosphorylation were increased in diabetic rodent hearts (26). Others have also found increased cTnI phosphorylation in diabetic animals (27, 28), which has led to the hypothesis that increased phosphorylation of cTnI reduces myofilament calcium sensitivity in the diabetic heart. However, no study has reported changes in myofilament calcium sensitivity that correspond with cTnI phosphorylation in the same diabetic samples. Moreover, the specific phospho-sites within the troponin complex, such as cTnI sites Ser23/24, threonine (Thr)144 and Ser150, have yet to be thoroughly studied in the diabetic heart. Therefore, while it is well-established that phosphorylation of cTnI can reduce myofilament calcium sensitivity (25, 29), this has not been conclusively established in the diabetic heart.

An additional post-translational modification, O-GlcNAcylation, is increased in the diabetic heart (30–32) and has also been shown to decrease calcium sensitivity (33). Upon the incubation of skinned trabeculae in GlcNAc, calcium sensitivity was reduced and myofilament proteins had increased OGlcNAcylation protein modification (33). Subsequent reduction of O-GlcNAcylation levels restored calcium sensitivity and occurred without differential phosphorylation of cTnI at Ser23/24 (33), the site responsible for reducing myofilament calcium sensitivity in other pathologies (29). Others have suggested that phosphorylation and O-GlcNAcylation may interact together; ‘competing’ for serine and threonine residues (30). It remains unclear how phosphorylation and O-GlcNAcylation interact within the diabetic heart or how these modifications together affect myofilament calcium sensitivity.

This study aimed to measure myofilament calcium sensitivity within the ZDF rat, a model previously shown to have impaired cardiac function caused by diabetes (21, 34). To determine if cardiomyocyte myofilament function changes throughout the time course of diabetes, we tested the calcium sensitivity of ZDF rats at 12 and 20 weeks of age. In addition, to identify potential mechanisms behind alterations in calcium sensitivity, we quantified total myofilament protein phosphorylation, O-GlcNAcylation and site-specific phosphorylation of cTnI. We hypothesized that: 1) myofilament calcium sensitivity would be reduced by 20 weeks of age in skinned diabetic cardiomyocytes, 2) protein phosphorylation would be augmented at cTnI, including phospho-site Ser23/24, and cTnT and 3) O-GlcNAc cTnI protein expression would be increased in diabetic cardiomyocytes.

Methods

Animals & Tissue Collection

Twelve and 20-week-old male type 2 diabetic Zucker Diabetic Fatty (DM) (ZDF $^{fa/fa}$, N = 10 per age group) rats and their lean non-diabetic (nDM) littermates (ZDF $^{+/+}$, N = 10 per age group) were used in this study. All experiments were approved and conducted within the guidelines of the Animal Ethics Committee of the University of Otago, New Zealand, and adhered to the NZ Animal Welfare Act of 1991, which complies with the US National Institutes of Health Guide for the Care and use of Laboratory Animals. Rats were euthanized with a lethal dose (60 mg/kg) of pentobarbital (Provit, Canada). Upon loss of orbital and

pedal reflexes, the chest cavity was opened and the heart was quickly excised and placed into a bath of cold relaxing buffer (100 mM potassium chloride, 1.75 mM ethylene glycol tetraacetic acid (EGTA), 10 mM Imidazole, 4 mM adenosine triphosphate magnesium, 5 mM magnesium chloride, pH 7.0 with potassium hydroxide). Heart and left ventricle (LV) weight were recorded and each chamber was dissected, quickly frozen in liquid nitrogen and stored at -80°C.

Echocardiography

Echocardiography was carried out at 12 and 20 weeks of age on nDM and DM rats using an echocardiography ultrasound machine (Vivid Q, General Electric Healthcare) to determine the effects of the progression of diabetes on systolic and diastolic left ventricular (LV) morphology and function. Rats were initially anaesthetized with 4% isoflurane in a gas chamber, and then transferred onto a heating pad. Anaesthesia was maintained at 2–3% isoflurane by nose cone during echocardiography. All exams were performed with the animal on its back and a shaven chest. Two-dimensional images were obtained from a parasternal long axis view. LV structure and systolic function was determined by measuring in M-mode. LV diastolic function was measured by pulse-wave Doppler images. To minimize the effects of isoflurane on the heart, echocardiography was performed two to three days prior to euthanasia to ensure washout.

Isolation of Rat Cardiomyocytes

Previously frozen LV samples were partially homogenized in relaxing buffer with HALT Protease and Phosphatase Inhibitor Cocktail 100X (Thermo Scientific, 78430). The myocyte suspension was centrifuged at 10000 rpm, re-suspended and permeabilized with 1.1% Triton X-100 detergent (Thermo Scientific, 28314) for 8 minutes. The resulting pellet of skinned myocytes was washed with relaxing buffer 3 times. Myocytes were stored on ice and used for up to two days, as previous studies found cells were equally viable for up to 48 hours (26, 35).

Cardiomyocyte Force Measurements

A single cardiomyocyte or small bundle of cells (approximately two to five) were mounted on an inverted phase contrast microscope (*Nikon*) and fixed between a piezoelectric motor and a force transducer (Aurora Scientific, 405 model) with the use of silicone glue (*Marineland Aquarium Sealant*) in a relaxing buffer. Stage temperature was set to 15°C and glue was left to cure for 30 minutes. Once cured, the cell could be moved into the well containing pCa 9.0 (lowest concentration of calcium) and stretched until the sarcomere length reached 2.3 um. Sarcomere length, cell length and cell height were visualized and measured using an *IDS* camera and *VSL 900B* software (Aurora Scientific).

The pCa_{50}, or the [calcium (Ca^{2+})] at which half-maximal tension was produced, is a measure of the calcium sensitivity of cardiomyocytes. Myofilament tension was developed by placing each cell into baths containing different concentrations of calcium (-log[Ca^{2+}] or pCa). Force was measured by slacking the myocyte by 20% of its original length (slack test). The force at a given pCa was measured as the change in force from peak length to 80% of initial length (0.8 L_o). Initially, force was measured in pCa 4.5 and then randomly selected submaximal pCa solutions, with every fourth or fifth activation made in 4.5

to assess any decline in myocyte performance. Submaximal pCa solutions were created by mixing different ratios of pCa 9.0 (EGTA 7mM, Imidazole 20 mM, magnesium chloride 5.42 mM, potassium chloride 79.16 mM, calcium chloride 16.33 uM, creatine phosphate 14.5 mM, magnesium adenosine triphosphate 4.74 mM) and 4.5 (EGTA 7mM, Imidazole 20 mM, magnesium chloride 5.26 mM, potassium chloride 64 mM, calcium chloride 7 mM, creatine phosphate 14.5 mM, magnesium adenosine triphosphate 4.81 mM), determined from the computer program Fabiato (36). The experimenter was blinded regarding whether a given cell was from a nDM or DM LV sample. Myocytes were excluded from data analysis if 80% of maximal force was not maintained by the end of the experimental protocol.

Maximal force, or the force at pCa 4.5 subtracted by the passive force measured at pCa 9.0, was normalized to the cross-sectional area (CSA) of the cell (CSA = 3.14*(cell width/2)^2). Active tension was calculated by subtracting passive tension at pCa 9.0 from the total tension measured by the slack test. Tension at each pCa was expressed as a fraction of the maximum tension (pCa 4.5) obtained for that cell under the same conditions. As described by Hofmann et al., data were analysed by least-squares regression using the Hill equation,

$$\text{Log}\,[(P_{rel})/(1 - P_{rel})] = n(\log\,[Ca^{2+}] + k)$$

where P_{rel} is tension expressed as a fraction of maximal tension, n is the Hill coefficient, and k is the intercept of the fitted line with the x-axis, which corresponds to the $[Ca^{2+}]$ at half-maximal (50%) tension (pCa_{50}) (37). With the use of constants derived from the Hill equation, tension data were fit using Prism software with the following Eq. (35).

$$P_{rel} = [Ca^{2+}]^n/(k^n + [Ca^{2+}]^n)$$

ProQ Diamond Phospho-Fluorescent Gel Staining

ProQ Diamond Phosphoprotein gel stain (Invitrogen, P33300) was used to determine myofilament protein phosphorylation from nDM and DM LV samples. Protein lysates were prepared by homogenizing the same LV samples used previously in RIPA buffer (sodium chloride 50 mM pH 7.4 with hydrogen chloride, sodium dodecyl sulfate (SDS) 1%, Triton X-100 1%, edetate disodium 1 mM). Protein samples (20 ug) were prepared for gel electrophoresis by adding 1X sample buffer, water and protein lysate of interest. Protein was denatured by heating at 95°C for 5 minutes and loaded onto a 4–20% gradient gel (BioRad, #4561096). A PeppermintStick Phosphoprotein Standard (Invitrogen, P27167) was used to identify myofilament proteins of interest and also as positive and negative controls for the phospho-staining technique. After gel electrophoresis was complete, gels were fixed overnight in 50% methanol and 10% acetic acid to remove remaining SDS. Gels were washed 3 times for a total of 30 minutes with ultrapure water to remove fix solution and subsequently stained with ProQ Diamond gel stain. Gels were protected from light, placed on shaker at 50 rpm and stained for 75 minutes. Next, gels were destained using ProQ Diamond Phosphoprotein Gel Destaining Solution (Invitrogen, P33310) for a total of 90 minutes. Each gel was then washed with ultrapure water before imaging on the VersaDoc Imager using a green light filter at 605 nm and exposed for 20 seconds.

Gels were then immersed in Sypro Ruby Protein Gel Stain (Invitrogen, S12000) overnight in the dark at 50 rpm to allow for the measurement of total protein and ensure equal loading across lanes. Before imaging, gels were washed in a Sypro Wash solution (10% methanol, 7% acetic acid) for 30 minutes and washed with ultrapure water. Sypro Ruby stained gels were imaged with the VersaDoc Imager using the UV Transilluminator filter at 605 nm and exposed for 1 second.

Gel band intensities were quantified using ImageStudio software (*LiCor* Tech). The amount of phosphorylation was normalized to total protein using a ratio of the signal intensity of the phospho-stained band divided by the signal intensity of the total protein at each respective protein of interest: cMyBP-C, cTnT, cTnI and myosin light chain II (MLCII). Due to high quantities of protein bands present near cTnT and cTnI bands, native cTnT and cTnI protein were run in neighboring lanes to confirm band identifies (Abcam, ab9937 & ab9936 respectively).

Western Blot Analysis of Phospho-Specific Proteins and O-GlcNAc

To measure the phosphorylation occurring at specific sites on cTnI, LV tissue was homogenized in RIPA buffer and protein lysates were prepared similarly to above. Proteins were separated on a 15% SDS PAGE gel and a molecular weight marker was used for protein identification (BioRad, 1610374). Each gel was run for approximately one hour at 120 V using a BioRad PowerPac blot system. Gels were then transferred onto a nitrocellulose membrane, 100 V for 90 minutes. After protein transfer, membranes were incubated in 5% milk powder TBST solution (Tris 50 mM, sodium chloride 150 mM, Tween-20 0.5%). Primary antibodies for total O-GlcNAc, cTnI and β-actin (loading control) were used (Abcam ab2739, ab4002, ab49900 respectively). All primary antibody incubations were performed overnight at 4°C. For secondary anti-rabbit and anti-mouse antibodies, incubation was for 1.5 hours at room temperature (Abcam ab97051 and ab97023 respectively).

After obtaining the total cTnI protein expression signal, the same membrane underwent a stripping protocol. To remove the cTnI antibody, a stripping buffer (β-mercaptoethanol 100mM, SDS 2%, Tris 62.8 mM pH 6.8) was used at 50°C for 30 minutes. Imaging was completed to confirm stripping of the membrane. Lastly, site-specific phosphorylation expression could be determined using one of the following primary antibodies: cTnI Ser 23/24, Thr 144 and Ser 150 (Cell Signaling 4004, Abcam ab58546 and ab169867 respectively). After an overnight incubation, membranes were washed with TBST and incubated with an anti-rabbit secondary antibody. To detect differences in cTnI phospho-specific levels we determined, for each sample, the signal intensity of phospho-cTnI site of interest normalized to total cTnI. To ensure equal loading, protein quantity was controlled by probing for and measuring β-actin signal intensity (Abcam, ab49900). To determine the amount of O-GlcNAc modified cTnI, total O-GlcNAc at the cTnI band was normalized to total cTnI expressed. All blots were imaged using the Syngene Imager after incubation with West Pico solution (ThermoFisher, 34580) to detect protein bands. Protein bands were analyzed using ImageJ Software or Image Studio software for total O-GlcNAc gel lanes.

Statistical Analysis

The four groups (12 nDM, 12 DM, 20 nDM and 20 DM) were compared using a two-way ANOVA and a Levene's test of normality was used to check for a normal distribution. An exception was made for site-specific western blotting, as experiments were completed at different time points (months apart) and made a two-way ANOVA comparison unfeasible. In this case, independent t-tests were run to compare 12-week-old nDM and DM rats and also 20-week-old nDM and DM rats and corrected by a Bonferroni's correction. Both SPSS (IBM) and Prism-8 (GraphPad) software were utilized to analyze and create figures, respectively. Statistical significance was set at $p \leq 0.05$.

Results

Animal Characteristics

DM rats, regardless of age, had higher blood glucose levels than nDM rats ($p < 0.0001$, Table 1) and hyperglycaemia was more severe with age ($p = 0.04$). Both 12- and 20-week-old DM rats were heavier than their nDM counterparts ($p < 0.0001$) and 20-week-old DM rats were heavier than 12week-old DM rats ($p < 0.0001$). There was no evidence of myocardial hypertrophy in DM rats (i.e., LV and heart weight were not significantly different across disease state), but 20-week-old rats had a greater heart weight to tibia length compared to 12-week-old rats, regardless of disease state ($p = 0.02$). The epididymal fat pad was greater in DM rats compared to nDM rats ($p < 0.0001$) and 20week-old DM rats had greater epididymal fat pad weight compared to 12-week-old DM rats ($p < 0.0001$).

Table 1
Descriptive Characteristics

Descriptive data table depicting body weight (g), blood glucose (mmol/L), heart and LV weight normalized to tibia length (g/cm), epididymal fat pad weight (g) and cell sample size. Cell sample size refers to the number of skinned cardiomyocytes used to analyze pCa_{50}. Two-way ANOVA, mean ± SEM, A = significant age effect, D = significant disease effect.

Characteristic Outcomes	12 nDM	12 DM	20 nDM	20 DM	Significance
Body Weight (g)	301.4 ± 15.7	351.1 ± 36.1	369.2 ± 13.6	403.1 ± 19.7	A, D
Blood Glucose (mmol/L)	11.5 ± 3.5	30.4 ± 2.0	12.9 ± 3.4	32.7 ± 1.7	A, D
Heart Weight / Tibia (g/cm)	0.32 ± 0.05	0.34 ± 0.04	0.36 ± 0.03	0.37 ± 0.04	A
LV Weight / Tibia (g/cm)	0.13 ± 0.01	0.14 ± 0.02	0.14 ± 0.02	0.15 ± 0.03	
Epididymal Fat Pad Weight (g)	0.96 ± 0.22	4.80 ± 0.53	1.35 ± 0.58	5.69 ± 0.54	A, D
Cell sample size	19	17	20	25	

Echocardiography

LV posterior wall thickness during systole (LVPWs) and diastole (LVPWd) were not different between nDM and DM rats (Table 2). Additionally, there was no significant effect of diabetes on end-diastolic volume (EDV), end-systolic volume (ESV) or ejection fraction (EF). Although, there was a significant effect of age on volumes, both EDV and ESV were greater in 20-week-old rats ($p = 0.006$ and $p = 0.005$, respectively). The E/A ratio, the ratio of peak early to late diastolic filling velocities, was not different between nDM and DM rats ($p = 0.8$).

Table 2
Echocardiography Variables

M-mode measurements (ejection fraction (%), fractional shortening (%), end-diastolic volume (EDV, mL), end-systolic volume (ESV, mL), heart rate (HR, bpm), LV poster wall dimensions in diastole and systole (LVPWd and LVPWs, cm)) and pulse-wave Doppler echocardiography measurements (E/A ratio, E velocity (m/s) and A velocity (m/s)) taken in the long-axis parasternal view. Two-way ANOVA, mean ± SEM, A = significant age effect.

Echocardiography Variables	12 nDM	12 DM	20 nDM	20 DM	
M Mode					
Ejection fraction (%)	77.5 ± 9.8	81.5 ± 4.9	76.4 ± 6.6	78.3 ± 5.8	A
Fractional shortening (%)	43.3 ± 9.3	46.1 ± 5.4	41.2 ± 5.9	43.2 ± 5.5	A
EDV (mL)	0.86 ± 0.4	0.88 ± 0.2	1.08 ± 0.3	1.20 ± 0.3	A
ESV (mL)	0.23 ± 0.2	0.17 ± 0.1	0.28 ± 0.1	0.28 ± 0.1	A
HR (bpm)	359.6 ± 46.1	336.6 ± 16.1	314.3 ± 15.0	302.6 ± 20.9	
LVPWd (cm)	0.18 ± 0.02	0.17 ± 0.02	0.18 ± 0.03	0.18 ± 0.01	
LVPWs (cm)	0.22 ± 0.03	0.21 ± 0.02	0.21 ± 0.03	0.23 ± 0.02	
Doppler					
E/A ratio	1.85 ± 0.51	1.88 ± 0.72	2.07 ± 0.51	2.16 ± 0.54	
E velocity (m/s)	0.63 ± 0.10	0.64 ± 0.14	0.58 ± 0.16	0.61 ± 0.14	
A velocity (m/s)	0.37 ± 0.09	0.38 ± 0.10	0.30 ± 0.07	0.30 ± 0.09	A

Skinned myocyte calcium sensitivity

Figure 2a & b displays the pCa-tension curves created for each group. pCa_{50} was greater in DM vs. nDM cardiomyocytes, regardless of age (Fig. 2c, $p = 0.0005$). In addition, 12-week-old rats had a greater pCa_{50} compared to 20-week-old rats (Fig. 2c, $p = 0.0001$). Maximal force and passive force were not significantly different between groups (Fig. 2d – e).

Total protein phosphorylation of key myofilament proteins

DM rats had less cTnI protein phosphorylation compared to nDM rats (p = 0.003, Fig. 3d). Twentyweek-old rats had significantly lower cTnT protein phosphorylation compared to 12weekold rats (p = 0.003, Fig. 3e) and although 20-week-old DM rats tended to have greater cTnT protein phosphorylation compared to 20-week-old nDM rats, the interaction was not statistically significant (p = 0.058). Phosphorylation of cMyBP-C nor MLCII were not different between nDM and DM rats (Fig. 3c & f). Additionally, when comparing the entire myocardium proteome, there were no significant differences between groups (Fig. 3f).

Phospho-specific cTnI antibodies

Four cTnI phospho-sites, Ser23/24, Thr144 and Ser150, were quantified by immunoblot due to their ability to affect pCa_{50} in health and disease (29). Twenty-week-old DM rats had reduced phosphorylation at Ser23/24 compared to 20-week-old nDM rats (p = 0.01, Fig. 4b), but there was no difference between groups at 12 weeks of age (Fig. 4a). There was no difference in Thr144 phosphorylation between DM and nDM rats (Fig. 4c – d). Ser150 phosphorylation tended to be higher in the 20-week-old DM rats compared to 20-week-old nDM rats (p = 0.055, Fig. 4f), but was not different between nDM and DM rats at 12 weeks of age (Fig. 4e).

O-GlcANacylation of the myocardium

Despite a reduction in protein phosphorylation of cTnI, there was no difference in the level of OGlcANacylated cTnI between DM and nDM rats (p = 0.11), but 20-week-old rats had greater cTnI OGlcNAc protein expression compared to 12-week-old rats (p = 0.003, Fig. 5b). Additionally, there tended to be greater amount of total myocardium O-GlcNAc expression (entire gel lane normalized to the β-actin signal) in DM groups vs. nDM groups, but this trend was not statistically significant (p = 0.07, Fig. 5a).

Discussion

There is a growing body of evidence indicating that altered calcium sensitivity contributes to cardiac dysfunction in diabetes (26, 33, 38). Both phosphorylation and O-GlcNAcylation of myofilament proteins alter cardiomyocyte calcium sensitivity and affect contractility (39–41); however, the changes in myofilament post-translational modifications, such as phosphorylation and O-GlcNAcylation, in diabetic hearts and the functional consequences of these changes are unclear. This study found that calcium sensitivity was increased and cTnI phosphorylation was reduced in both 12 and 20-week-old DM rat hearts, refuting our initial hypothesis. cTnI protein phosphorylation at residues Ser23/24 was significantly reduced in DM rats at 20 weeks of age, which is consistent with increased calcium sensitivity (29). We found no change in O-GlcNAcylated myocardium proteins between nDM and DM rats. These findings confirm that diabetes alters the phosphorylation and calcium sensitivity of myofilament proteins, but the direction appears to be dependent on the model of diabetes being tested.

Calcium sensitivity within the DM heart

Contrary to our initial hypothesis, pCa_{50} was greater in skinned cardiomyocytes from DM rat hearts than their nDM littermates. This outcome was surprising because we (42) and others (26) had found, using a similar methodology, that calcium sensitivity was reduced in human diabetic myofilaments. The discrepancy in our findings may reflect inherent differences between human and rodent cardiomyocytes. Animal models of diabetes report unchanged (43), reduced (33) and, as indicated in this study, increased (38, 44) calcium sensitivity. The opposing calcium sensitivity results between rodent and human cardiac myofilaments has been attributed to species-specific differences in post-translational modifications, particularly phosphorylation, of myofilament proteins (45); however, these differences have not been conclusively associated with altered phosphorylation within diabetic samples.

cTnI phosphorylation alters calcium sensitivity

A somewhat unanticipated finding was that diabetes changed cTnI protein phosphorylation in ways associated with increased calcium sensitivity. We predicted that DM rats would have reduced pCa_{50}, which previous studies have associated with increased phosphorylation of total cTnI and cTnI Ser23/24 and reduced phosphorylation of cTnI Ser150 (29, 46, 47). Instead we found that total cTnI protein phosphorylation and Ser23/24 phosphorylation were *reduced* in 20-week-old DM rat hearts. We found a large, but statistically insignificant ($p = 0.055$), *increase* in phosphorylation of Ser150. While these findings refute our experimental hypothesis, and contradict findings in human cells, the increase of pCa_{50} and 'coordinated' phosphorylation of cTnI, suggests that diabetes-induced post-translational modifications of cTnI impacts the function of the diabetic cardiomyocyte.

The well-studied Ser23/24 residues on cTnI are common targets of protein kinase A (PKA), which is mediated by β-adrenergic receptor (AR) stimulation (48). Upon β_1-AR stimulation, a G_s-protein-mediated intracellular cascade activates PKA, which phosphorylates cTnI at Ser23/24 (49–52). We did not measure PKA protein expression, however β_1-AR and G_s-protein expression are reduced in the ZDF DM rat (34), which suggests that there is less PKA-specific phosphorylation in the 20 week-old ZDF DM rat. In contrast, cTnI Ser150 phosphorylation is a target of p21 activated kinase 3 (PAK3) and when phosphorylated results in increased myofilament calcium sensitivity (46). PAK's have been shown to have increased expression in myocytes under stress (53) and have elevated cardiac expression in diabetes (54). Given that this site is known to sensitize the myofilament proteins, an increased pCa_{50} within DM rats might be explained with increased phosphorylation at Ser150. However, at 12 weeks of age, there was no difference in phosphorylation at this site casting doubt over its functional significance.

The functional effects of Thr144 phosphorylation is not well-understood. Studies have found both increased (55) and unchanged myofilament sensitivity to calcium (56) upon the phosphorylation of Thr144. An alternative hypothesis is that the functional consequences of phosphorylated Thr144 might be dependent on communicating with other key cTnI phospho-sites, including Ser43/45 (57). The authors found phospho-mimetic Thr144 attenuated the "breaking" effects (e.g., reduced force production) of phospho-Ser43/45 (58), resulting in accelerated time to peak shortening and time to 50% re-lengthening

(57). These results further support the hypothesis that multiple phospho-sites on cTnI might interact together and affect cellular function.

Total protein phosphorylation of other myofilament proteins

We did not find much evidence that diabetes affected the amount of phosphorylation of other key myofilament proteins (cMyBP-C, cTnT and MLCII) known to alter pCa_{50} (59–61). Phosphorylation of cTnT, the troponin subunit responsible for binding to tropomyosin (22), was greater in 12 vs. 20-week-old rats. cTnT phosphorylation, a protein kinase C (PKC) target, has been shown to decrease maximal force and calcium sensitivity (56). Our 12-week-old rats had a greater pCa_{50} compared to 20-week-old rats, which cannot be explained by the increase in cTnT phosphorylation. Additionally, we found no significant difference in maximal force between groups, which is supported by our lack of altered cTnT phosphorylation expression between nDM and DM rats. cMyBP-C and MLCII phosphorylation were not different between DM and nDM rats and thus we believe it is unlikely these myofilament proteins are contributing significantly to the increase in calcium sensitivity found in this study.

O-GlcNAcylation in the diabetic heart

O-GlcNAc modifications of myocardium proteins are augmented in diabetes (62) and global myofilament O-GlcNAcylation has been shown to reduce calcium sensitivity, without any change in Ser23/24 phosphorylation, in a STZ rat model of diabetes (33). Additionally, an emerging hypothesis is that O-GlcNAc competes with phosphorylation for the modification of serine and threonine residues (30). Despite this, we found no difference in the amount of O-GlcNAcylation at cTnI between nDM and DM groups, but cTnI O-GlcNAc protein expression was greater in 20 vs. 12-week-old rats. Additionally, there was no significant difference in the total O-GlcNAc protein expression between nDM and DM rats ($p = 0.07$). These results are surprising, especially given the severity of the hyperglycaemia quantified, but unlike the previous study described (33), we had a decrease in cTnI Ser23/24 phosphorylation, which appears to be driving the increase in calcium sensitivity.

Change in cellular function occurred without any change in echocardiography variables

Echocardiography variables measuring LV structure (e.g., LVPWd & LVPWs), volume (e.g., EDV, ESV), systolic function (e.g., EF) and diastolic function (e.g., E/A) were not different between nDM and DM rats (Table 2). These data are consistent with previous findings from our group, which indicated that ZDF rats have preserved EF and no evidence of advanced heart failure (21). The lack of evidence for organ-level structural or functional changes is surprising when considering that our cellular data indicated an increased myofilament calcium sensitivity. An increase in calcium sensitivity is thought to improve systolic function and/or impair diastolic function, therefore it is surprising that we found no change in any echocardiography outcome variables. An implication of these results might be that increased pCa_{50} is a compensatory mechanism for the maintenance of systolic function within DM rat hearts. This is a difficult hypothesis to test directly and therefore we can only suggest the possibility of this outcome.

Limitations

The ZDF rat develops hyperglycaemia and obesity due to a leptin receptor mutation (63). Leptin, the hormone responsible for sensing hunger, is an important metabolic regulator (64). Therefore, a valid critique of this model would be the potential to affect other metabolic signalling pathways. Leptin has been shown to reduce cardiac hypertrophy and apoptosis and raise both blood pressure and heart rate (65), which might explain, at least in-part, heterogeneity in the pCa_{50} results reported across various models. Despite this, the ZDF rat is a widely used model of type-II diabetes due to its ability to model the type-II diabetic phenotype: hyperinsulinemia, hyperglycaemia and hyperlipidaemia without evidence of increased blood pressure, hypertrophy and other factors known to cause cardiovascular disease independently of diabetes.

Conclusion

This study found that DM cardiomyocytes from ZDF rats have increased calcium sensitivity and reduced cTnI phosphorylation. The decrease in phosphorylation at cTnI Ser23/24 support these findings, given it is well-accepted that increased pCa_{50} is a consequence of less phosphorylation at Ser23/24. Although this study cannot prove causation, these data indicate that cTnI phosphorylation plays an important role in the alteration of single cell function in the diabetic heart. Despite finding increased calcium sensitivity in diabetic cardiomyocytes, we found no evidence of LV systolic, structural nor diastolic dysfunction, which might be compensatory to maintain systolic function, but might also be costly to diastolic function as the disease progresses. In conclusion, this study highlights the complexity of the myofilament proteome and its ability to alter cardiomyocyte function within the diabetic heart.

Abbreviations

AR

adrenergic receptor; Calcium:Ca^{2+}; Calcium sensitivity:pCa_{50}; CaMKII:calcium/calmodulin-dependent protein kinase; cMyBP-C:cardiac myosin binding protein-C; CSA:cross-sectional area; cTnI:cardiac troponin I; cTnT:cardiac troponin T; DM:diabetic; E/A:ratio of peak early to late diastolic filling velocities; EDV:end-diastolic volume; ESD:end-systolic volume; EGTA:ethylene glycol tetraacetic acid; F_{max}:maximal force; $F_{passive}$:passive force; L_o:initial length; LV:left ventricle; LVPWd:LV posterior wall thickness during diastole; LVPWs:LV posterior wall thickness during systole; MLCII:myosin light chain II; nDM:non-diabetic; PAK3:p21 activated kinase 3; PKA:protein kinase A; PKC:protein kinase C; PLB:phospholamban; SDS:sodium dodecyl sulfate; SERCA:sarcoplasmic reticulum Ca^{2+}-ATPase; Ser:serine; Thr:Threonine; ZDF:Zucker Diabetic Fatty;

Declarations

Ethics approval

All animal studies were approved by the University of Otago Animal Ethics Committee (AUP-18-50) and were conducted in accordance with the New Zealand Animal Welfare Act (1999).

Consent for publication

Not Applicable

Availability of data and materials

The datasets used and/or analyzed during the current study are available from the corresponding author on reasonable request.

Competing interests

The authors have no competing interests to declare.

Funding

This publication was completed with support from the Southland Medial Foundation and the Health Research Council (18/693).

Authors' contributions

JCB is the guarantor of this work and had full access to all the data in the study, taking responsibility for the integrity of the data and accuracy of the data analysis. ACG designed and performed all animal experiments, analyzed data and wrote the paper. OMSG and AP aided with animal handling and data collection. JCB, JRE, GMD, AP reviewed and edited the manuscript. JCB, GTW, JRE, GMD funded the study. All authors approved the final manuscript.

Acknowledgements

The authors wish to thank Dr. Carol Bussey (University of Otago) and Rachel Wallace (University of Otago) for sharing their echocardiography and immunoblotting protocols.

References

1. Diamant M, Lamb HJ, Groeneveld Y, Endert EL, Smit JWA, Bax JJ, et al. Diastolic dysfunction is associated with altered myocardial metabolism in asymptomatic normotensive patients with well-controlled type 2 diabetes mellitus. J Am Coll Cardiol. 2003 Jul 16;42(2):328–35.
2. From AM, Scott CG, Chen HH. The development of heart failure in patients with diabetes mellitus and pre-clinical diastolic dysfunction a population-based study. J Am Coll Cardiol. 2010 Jan 26;55(4):300–5.
3. van Heerebeek L, Hamdani N, Handoko ML, Falcao-Pires I, Musters RJ, Kupreishvili K, et al. Diastolic stiffness of the failing diabetic heart: importance of fibrosis, advanced glycation end products, and

myocyte resting tension. Circulation. 2008 Jan 1;117(1):43–51.

4. Jain A, Avendano G, Dharamsey S, Dasmahapatra A, Agarwal R, Reddi A, et al. Left ventricular diastolic function in hypertension and role of plasma glucose and insulin. Comparison with diabetic heart. Circulation. 1996 Apr 1;93(7):1396–402.
5. Rutter MK, Parise H, Benjamin EJ, Levy D, Larson MG, Meigs JB, et al. Impact of glucose intolerance and insulin resistance on cardiac structure and function: sex-related differences in the Framingham Heart Study. Circulation. 2003 Jan 28;107(3):448–54.
6. Zarich SW, Arbuckle BE, Cohen LR, Roberts M, Nesto RW. Diastolic abnormalities in young asymptomatic diabetic patients assessed by pulsed Doppler echocardiography. J Am Coll Cardiol. 1988 Jul;12(1):114–20.
7. Boonman-de Winter LJM, Rutten FH, Cramer MJM, Landman MJ, Liem AH, Rutten GEHM, et al. High prevalence of previously unknown heart failure and left ventricular dysfunction in patients with type 2 diabetes. Diabetologia. 2012 Aug;55(8):2154–62.
8. Bouthoorn S, Gohar A, Valstar G, den Ruijter HM, Reitsma JB, Hoes AW, et al. Prevalence of left ventricular systolic dysfunction and heart failure with reduced ejection fraction in men and women with type 2 diabetes mellitus: a systematic review and meta-analysis. Cardiovasc Diabetol. 2018 18;17(1):58.
9. Gusso S, Hofman P, Lalande S, Cutfield W, Robinson E, Baldi JC. Impaired stroke volume and aerobic capacity in female adolescents with type 1 and type 2 diabetes mellitus. Diabetologia. 2008 Jul;51(7):1317–20.
10. Soliman OII, van Dalen BM, Theuns DAMJ, ten Cate FJ, Nemes A, Jordaens LJ, et al. The ischemic etiology of heart failure in diabetics limits reverse left ventricular remodeling after cardiac resynchronization therapy. J Diabetes Complications. 2009 Oct;23(5):365–70.
11. Sutton MGSJ, Plappert T, Hilpisch KE, Abraham WT, Hayes DL, Chinchoy E. Sustained reverse left ventricular structural remodeling with cardiac resynchronization at one year is a function of etiology: quantitative Doppler echocardiographic evidence from the Multicenter InSync Randomized Clinical Evaluation (MIRACLE). Circulation. 2006 Jan 17;113(2):266–72.
12. Kannel WB, Hjortland M, Castelli WP. Role of diabetes in congestive heart failure: the Framingham study. Am J Cardiol. 1974 Jul;34(1):29–34.
13. Nichols GA, Gullion CM, Koro CE, Ephross SA, Brown JB. The incidence of congestive heart failure in type 2 diabetes: an update. Diabetes Care. 2004 Aug;27(8):1879–84.
14. Stratton IM, Adler AI, Neil HA, Matthews DR, Manley SE, Cull CA, et al. Association of glycaemia with macrovascular and microvascular complications of type 2 diabetes (UKPDS 35): prospective observational study. BMJ. 2000 Aug 12;321(7258):405–12.
15. Bugger H, Abel ED. Molecular mechanisms of diabetic cardiomyopathy. Diabetologia. 2014 Apr 1;57(4):660–71.
16. Pereira L, Ruiz-Hurtado G, Rueda A, Mercadier J-J, Benitah J-P, Gómez AM. Calcium signaling in diabetic cardiomyocytes. Cell Calcium. 2014 Nov 1;56(5):372–80.

17. Belke DD, Swanson EA, Dillmann WH. Decreased Sarcoplasmic Reticulum Activity and Contractility in Diabetic db/db Mouse Heart. Diabetes. 2004 Dec 1;53(12):3201–8.
18. Pereira L, Matthes J, Schuster I, Valdivia HH, Herzig S, Richard S, et al. Mechanisms of [Ca2+]i transient decrease in cardiomyopathy of db/db type 2 diabetic mice. Diabetes. 2006 Mar;55(3):608–15.
19. Yaras N, Ugur M, Ozdemir S, Gurdal H, Purali N, Lacampagne A, et al. Effects of Diabetes on Ryanodine Receptor Ca Release Channel (RyR2) and Ca2+ Homeostasis in Rat Heart. Diabetes. 2005 Nov 1;54(11):3082–8.
20. Lamberts RR, Lingam SJ, Wang H-Y, Bollen IAE, Hughes G, Galvin IF, et al. Impaired relaxation despite upregulated calcium-handling protein atrial myocardium from type 2 diabetic patients with preserved ejection fraction. Cardiovasc Diabetol. 2014 Apr 5;13:72.
21. Daniels LJ, Wallace RS, Nicholson OM, Wilson GA, McDonald FJ, Jones PP, et al. Inhibition of calcium/calmodulin-dependent kinase II restores contraction and relaxation in isolated cardiac muscle from type 2 diabetic rats. Cardiovasc Diabetol. 2018 Jun 14;17(1):89.
22. Solaro RJ, Kobayashi T. Protein phosphorylation and signal transduction in cardiac thin filaments. J Biol Chem. 2011 Mar 25;286(12):9935–40.
23. Solaro RJ, Moir AJ, Perry SV. Phosphorylation of troponin I and the inotropic effect of adrenaline in the perfused rabbit heart. Nature. 1976 Aug 12;262(5569):615–7.
24. Winegrad Saul. Cardiac Myosin Binding Protein C. Circ Res. 1999 May 28;84(10):1117–26.
25. Marston SB, de Tombe PP. Point/Counterpoint Troponin phosphorylation and myofilament Ca2+-sensitivity in heart failure: increased or decreased? J Mol Cell Cardiol. 2008 Nov;45(5):603–7.
26. Jweied EE, McKinney RD, Walker LA, Brodsky I, Geha AS, Massad MG, et al. Depressed cardiac myofilament function in human diabetes mellitus. Am J Physiol-Heart Circ Physiol. 2005 Dec 1;289(6):H2478–83.
27. Liu X, Takeda N, Dhalla NS. Troponin I phosphorylation in heart homogenate from diabetic rat. Biochim Biophys Acta. 1996 Jun 7;1316(2):78–84.
28. Malhotra A, Reich D, Reich D, Nakouzi A, Sanghi V, Geenen DL, et al. Experimental diabetes is associated with functional activation of protein kinase C epsilon and phosphorylation of troponin I in the heart, which are prevented by angiotensin II receptor blockade. Circ Res. 1997 Dec;81(6):1027–33.
29. Layland J, Solaro RJ, Shah AM. Regulation of cardiac contractile function by troponin I phosphorylation. Cardiovasc Res. 2005 Apr 1;66(1):12–21.
30. Hart GW, Slawson C, Ramirez-Correa G, Lagerlof O. Cross talk between O-GlcNAcylation and phosphorylation: roles in signaling, transcription, and chronic disease. Annu Rev Biochem. 2011;80:825–58.
31. Ramirez-Correa GA, Jin W, Wang Z, Zhong X, Gao WD, Dias WB, et al. O-linked GlcNAc Modification of Cardiac Myofilament Proteins: A Novel Regulator of Myocardial Contractile Function. Circ Res. 2008 Dec 5;103(12):1354–8.

32. Yang X, Qian K. Protein O-GlcNAcylation: emerging mechanisms and functions. Nat Rev Mol Cell Biol. 2017;18(7):452–65.
33. Ramirez-Correa GA, Ma J, Slawson C, Zeidan Q, Lugo-Fagundo NS, Xu M, et al. Removal of Abnormal Myofilament O-GlcNAcylation Restores Ca2+ Sensitivity in Diabetic Cardiac Muscle. Diabetes. 2015 Oct;64(10):3573–87.
34. Thaung HPA, Baldi JC, Wang H-Y, Hughes G, Cook RF, Bussey CT, et al. Increased Efferent Cardiac Sympathetic Nerve Activity and Defective Intrinsic Heart Rate Regulation in Type 2 Diabetes. Diabetes. 2015 Aug 1;64(8):2944–56.
35. Diffee GM, Seversen EA, Titus MM. Exercise training increases the Ca2+sensitivity of tension in rat cardiac myocytes. J Appl Physiol. 2001 Jul 1;91(1):309–15.
36. Fabiato A. Computer programs for calculating total from specified free or free from specified total ionic concentrations in aqueous solutions containing multiple metals and ligands. Methods Enzymol. 1988;157:378–417.
37. Hofmann PA, Hartzell HC, Moss RL. Alterations in Ca2+ sensitive tension due to partial extraction of C-protein from rat skinned cardiac myocytes and rabbit skeletal muscle fibers. J Gen Physiol. 1991 Jun 1;97(6):1141–63.
38. Falcão-Pires I, Palladini G, Gonçalves N, van der Velden J, Moreira-Gonçalves D, Miranda-Silva D, et al. Distinct mechanisms for diastolic dysfunction in diabetes mellitus and chronic pressure-overload. Basic Res Cardiol. 2011 Sep;106(5):801–14.
39. Bilchick KC, Duncan JG, Ravi R, Takimoto E, Champion HC, Gao WD, et al. Heart failure-associated alterations in troponin I phosphorylation impair ventricular relaxation-afterload and force-frequency responses and systolic function. Am J Physiol Heart Circ Physiol. 2007 Jan;292(1):H318-325.
40. Hart GW, Housley MP, Slawson C. Cycling of O-linked beta-N-acetylglucosamine on nucleocytoplasmic proteins. Nature. 2007 Apr 26;446(7139):1017–22.
41. Murphy AM. Heart failure, myocardial stunning, and troponin: a key regulator of the cardiac myofilament. Congest Heart Fail Greenwich Conn. 2006 Feb;12(1):32–8; quiz 39–40.
42. Baldi C, Erickson J, Wallace R, Wilkins G, Diffee G. Reduced calcium sensitivity of diabetic human cardiomyocytes: The role of cTnI phosphorylation. Poster presented at: Myofilament Conference; 2018 May.
43. van den Brom CE, Huisman MC, Vlasblom R, Boontje NM, Duijst S, Lubberink M, et al. Altered myocardial substrate metabolism is associated with myocardial dysfunction in early diabetic cardiomyopathy in rats: studies using positron emission tomography. Cardiovasc Diabetol. 2009 Jul 22;8:39.
44. Mellor KM, Wendt IR, Ritchie RH, Delbridge LMD. Fructose diet treatment in mice induces fundamental disturbance of cardiomyocyte Ca2+ handling and myofilament responsiveness. Am J Physiol-Heart Circ Physiol. 2011 Dec 23;302(4):H964–72.
45. Hamdani N, de Waard M, Messer AE, Boontje NM, Kooij V, van Dijk S, et al. Myofilament dysfunction in cardiac disease from mice to men. J Muscle Res Cell Motil. 2008;29(6–8):189–201.

46. Buscemi N, Foster DB, Neverova I, Van Eyk JE. p21-activated kinase increases the calcium sensitivity of rat triton-skinned cardiac muscle fiber bundles via a mechanism potentially involving novel phosphorylation of troponin I. Circ Res. 2002 Sep 20;91(6):509–16.
47. Solaro RJ, van der Velden J. Why does troponin I have so many phosphorylation sites? Fact and Fancy. J Mol Cell Cardiol. 2010 May;48(5):810–6.
48. Fentzke RC, Buck SH, Patel JR, Lin H, Wolska BM, Stojanovic MO, et al. Impaired cardiomyocyte relaxation and diastolic function in transgenic mice expressing slow skeletal troponin I in the heart. J Physiol. 1999 May 15;517 (Pt 1):143–57.
49. Bers D. Cardiac excitation–contraction coupling | Nature [Internet]. 2002 [cited 2018 Aug 15]. Available from: https://www.nature.com/articles/415198a
50. Kentish JC, McCloskey DT, Layland J, Palmer S, Leiden JM, Martin AF, et al. Phosphorylation of troponin I by protein kinase A accelerates relaxation and crossbridge cycle kinetics in mouse ventricular muscle. Circ Res. 2001 May 25;88(10):1059–65.
51. Swiderek K, Jaquet K, Meyer HE, Schächtele C, Hofmann F, Heilmeyer LM. Sites phosphorylated in bovine cardiac troponin T and I. Characterization by 31P-NMR spectroscopy and phosphorylation by protein kinases. Eur J Biochem. 1990 Jul 5;190(3):575–82.
52. Zhang R, Zhao J, Potter JD. Phosphorylation of both serine residues in cardiac troponin I is required to decrease the Ca2+ affinity of cardiac troponin C. J Biol Chem. 1995 Dec 22;270(51):30773–80.
53. Seko Y, Takahashi N, Tobe K, Kadowaki T, Yazaki Y. Hypoxia and hypoxia/reoxygenation activate p65PAK, p38 mitogen-activated protein kinase (MAPK), and stress-activated protein kinase (SAPK) in cultured rat cardiac myocytes. Biochem Biophys Res Commun. 1997 Oct 29;239(3):840–4.
54. Raut SK, Kumar A, Singh GB, Nahar U, Sharma V, Mittal A, et al. miR-30c Mediates Upregulation of Cdc42 and Pak1 in Diabetic Cardiomyopathy. Cardiovasc Ther. 2015 Jun;33(3):89–97.
55. Wang H, Grant JE, Doede CM, Sadayappan S, Robbins J, Walker JW. PKC-betaII sensitizes cardiac myofilaments to Ca2+ by phosphorylating troponin I on threonine-144. J Mol Cell Cardiol. 2006 Nov;41(5):823–33.
56. Sumandea MP, Burkart EM, Kobayashi T, De Tombe PP, Solaro RJ. Molecular and integrated biology of thin filament protein phosphorylation in heart muscle. Ann N Y Acad Sci. 2004 May;1015:39–52.
57. Lang SE, Stevenson TK, Schatz TM, Biesiadecki BJ, Westfall MV. Functional communication between PKC-targeted cardiac troponin I phosphorylation sites. Arch Biochem Biophys. 2017 01;627:1–9.
58. Lang SE, Schwank J, Stevenson TK, Jensen MA, Westfall MV. Independent Modulation of Contractile Performance by Cardiac Troponin I Ser43 and Ser45 in the Dynamic Sarcomere. J Mol Cell Cardiol. 2015 Feb;79:264–74.
59. Streng AS, de Boer D, van der Velden J, van Dieijen-Visser MP, Wodzig WKWH. Posttranslational modifications of cardiac troponin T: An overview. J Mol Cell Cardiol. 2013 Oct 1;63:47–56.
60. Tong CW, Nair NA, Doersch KM, Liu Y, Rosas PC. Cardiac myosin-binding protein-C is a critical mediator of diastolic function. Pflugers Arch. 2014;466(3):451–7.

61. Warren SA, Briggs LE, Zeng H, Chuang J, Chang EI, Terada R, et al. Myosin light chain phosphorylation is critical for adaptation to cardiac stress. Circulation. 2012 Nov 27;126(22):2575–88.
62. Ma J, Hart GW. Protein O-GlcNAcylation in diabetes and diabetic complications. Expert Rev Proteomics. 2013 Aug;10(4):365–80.
63. Phillips MS, Liu Q, Hammond HA, Dugan V, Hey PJ, Caskey CT, et al. Leptin receptor missense mutation in the fatty Zucker rat. Nat Genet. 1996 May;13(1):18–9.
64. Kelesidis T, Kelesidis I, Chou S, Mantzoros CS. Narrative Review: The Role of Leptin in Human Physiology: Emerging Clinical Applications. Ann Intern Med. 2010 Jan 19;152(2):93–100.
65. Hall ME, Harmancey R, Stec DE. Lean heart: Role of leptin in cardiac hypertrophy and metabolism. World J Cardiol. 2015 Sep 26;7(9):511–24.

Figures

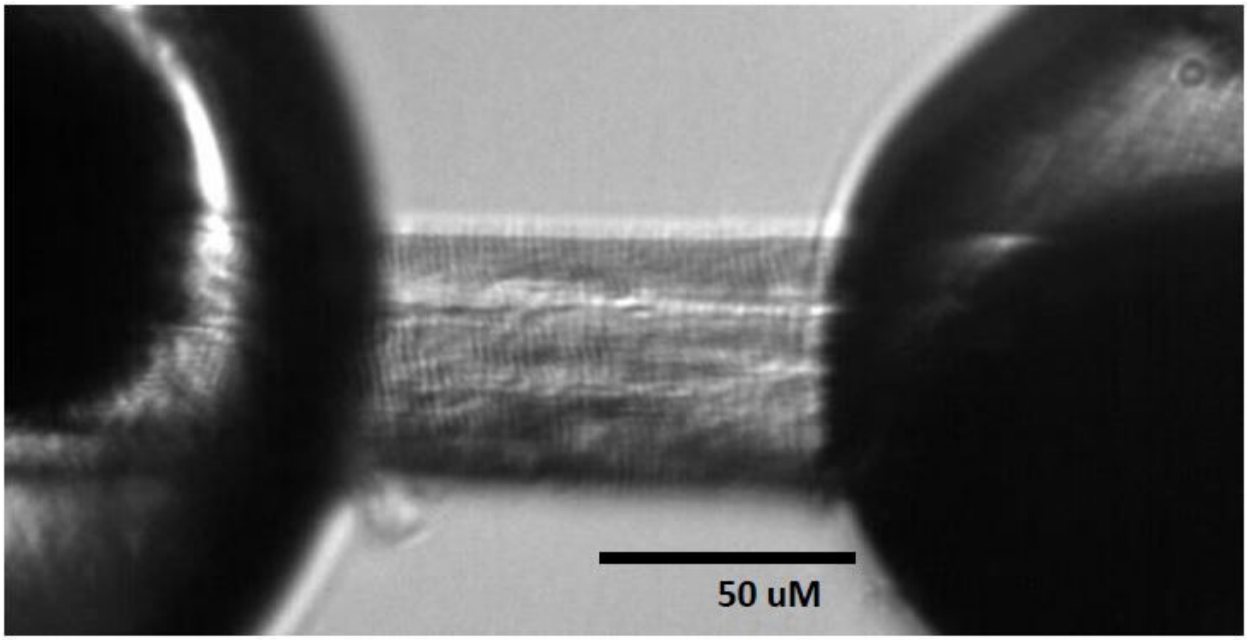

Figure 1

Example of a single skinned cardiomyocyte attached to two pins with silicone glue at 10X magnification. The left pin attaches to the force-transducer and the right pin attached to the piezoelectric motor, which allows the pin to move for slack tests.

Figure 2

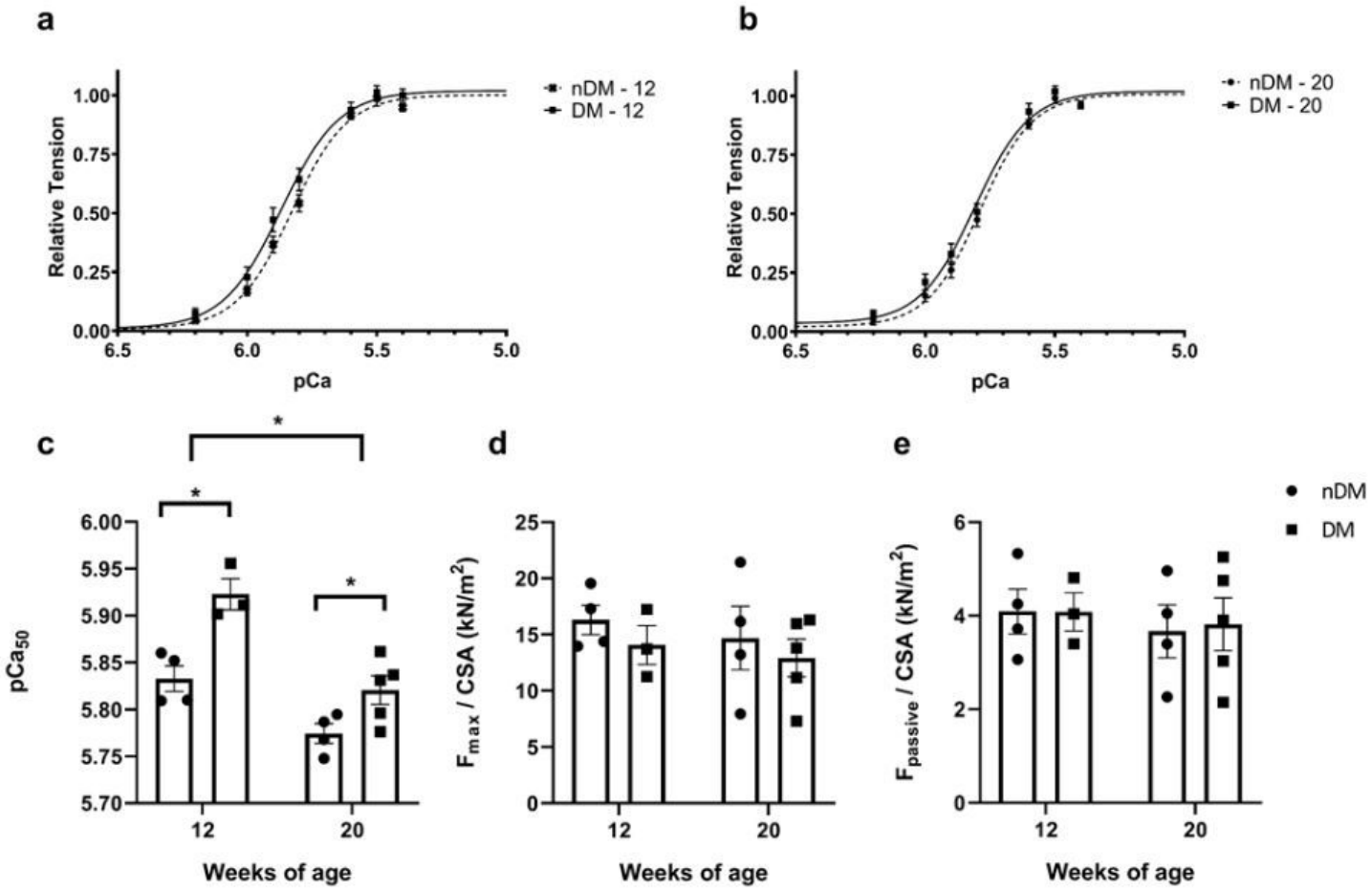

Figure 2

(a-b) pCa-tension curves generated by normalizing force at each pCa to maximal force measured in pCa 4.5 for 12- and 20-week-old ZDF rats respectively. (c) pCa50 values across groups. (d) Maximal force (Fmax), force at pCa 4.5 subtracted by the passive force at pCa 9.0, in each group. (e) Passive force (Fpassive) for each group. Two-way ANOVA, mean ± SEM, N = 3-5 hearts/group, n = 4-5 cells/heart.

Figure 3

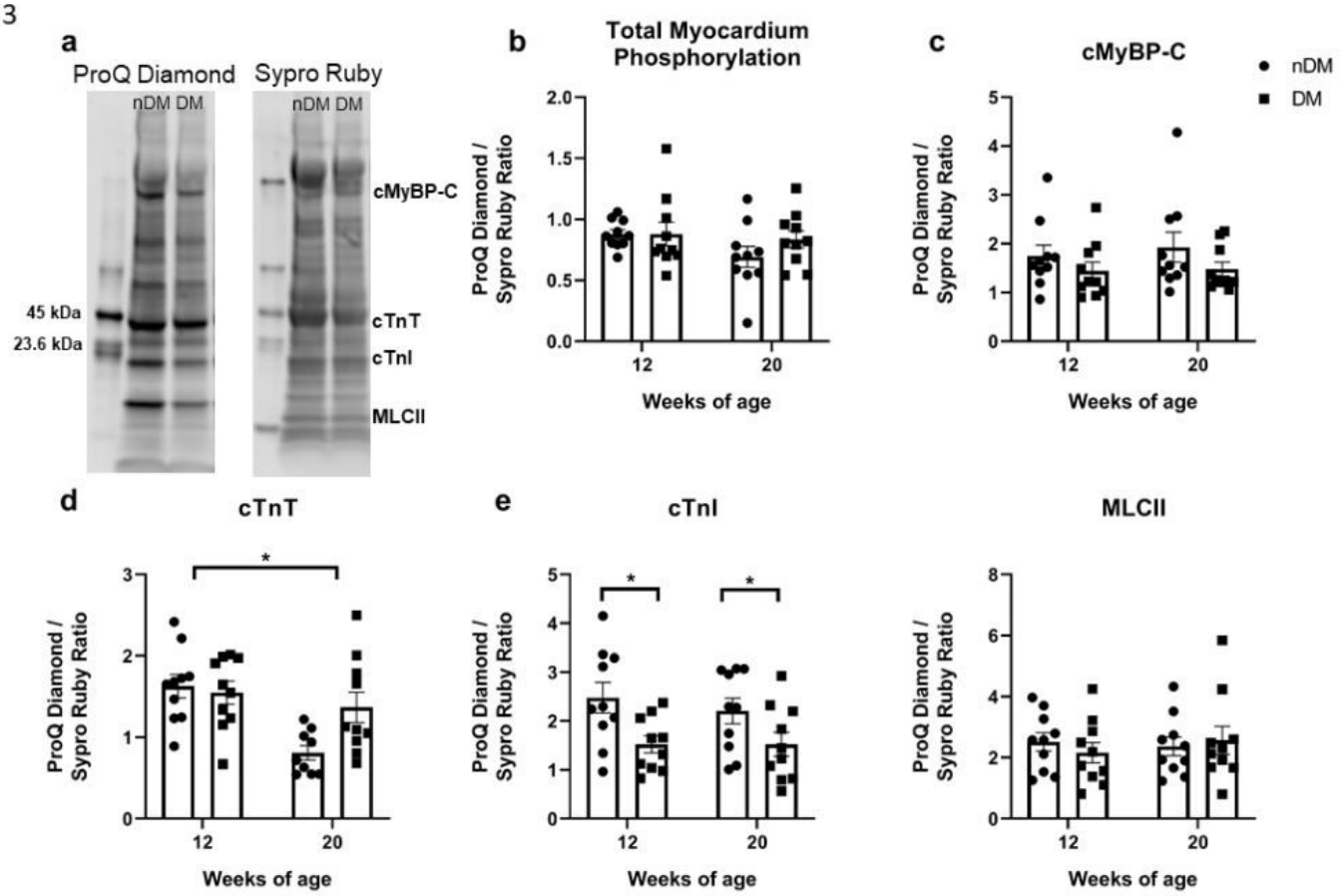

Figure 3

(a) Example of ProQ Diamond stained gradient gel and downstream Sypro Ruby gel staining. Ratio of ProQ Diamond signal to Sypro Ruby signal for (b) the total myocardium proteome phosphorylation (c) cMyBP-C (d) cTnT, (e) cTnI, and (f) MLCII. Two-way ANOVA, mean ± SEM.

Figure 4

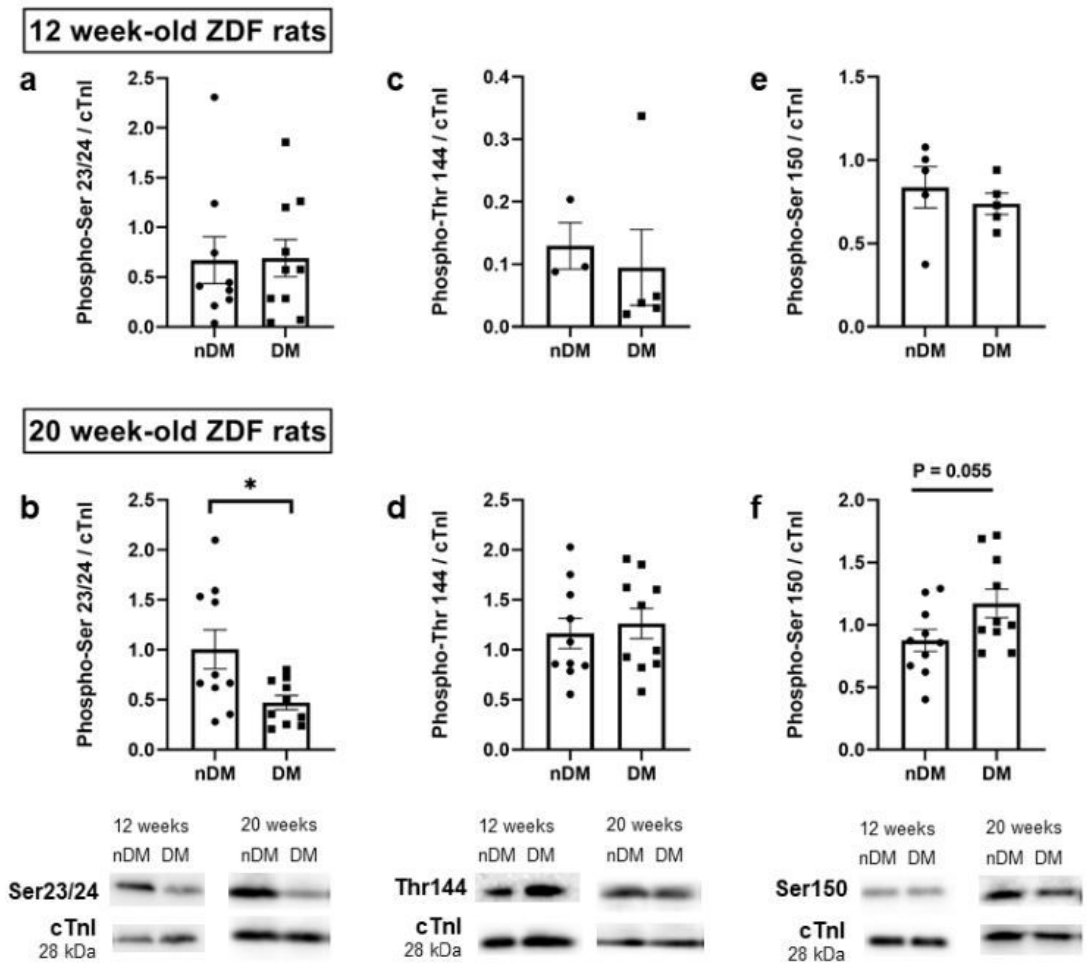

Figure 4

Phospho-specific cTnI antibodies to determine which residues were responsible for the overall change in cTnI phosphorylation. (a & b) Ser23/24 examples blots normalized to cTnI protein. (c & d) Thr144 example blots normalized to cTnI. (e & f) Ser150 example blots normalized to cTnI. Representative gels at each respective phospho-site compared to the total cTnI protein. Mean ± SEM, t-test.

Figure 5

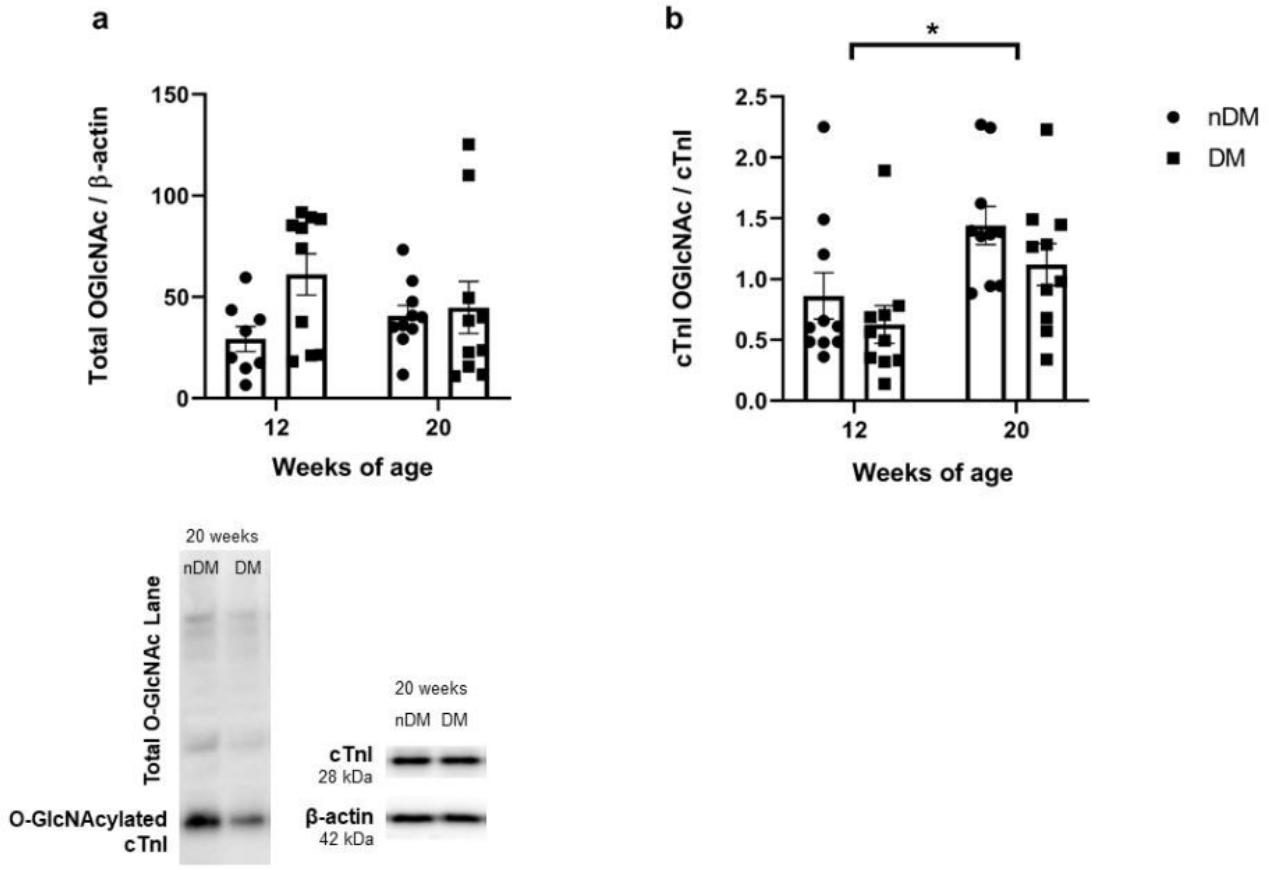

Figure 5

(a) The amount of O-GlcNAc in the entire gel lane or myocardium proteome relative to β-actin. (b) The ratio of O-GlcNAc occurring at cTnI relative to the total cTnI protein loaded. (c) Representative gels of O-GlcNAc, cTnI and β-actin. Two-way ANOVA, mean ± SEM.